

# Dopant and carrier concentration in Si in equilibrium with monoclinic SiP precipitates

S. Solmi, A. Parisini, R. Angelucci, and A. Armigliato

CNR-Istituto di Chimica e Tecnologia dei Materiali e Componenti per l'Elettronica (LAMEL), Via P. Gobetti, 101-40129 Bologna, Italy

D. Nobili

Dipartimento di Chimica Applicata e Scienza dei Materiali, University of Bologna, Bologna, Italy

L. Moro

Centro Materiali e Biofisica Medica (CMBM), 38050 Povo, Italy

(Received 20 July 1995; revised manuscript received 22 November 1995)

The behavior of silicon slices very heavily implanted ( $1.5 \times 10^{17} \text{ cm}^{-2}$ ) with phosphorus was investigated by transmission electron microscopy and secondary neutral mass spectrometry (SNMS) after annealing at 800, 850, 900, and 1000 °C. Precipitation of large monoclinic, and partially orthorhombic, SiP particles takes place in the most heavily doped region. From the shape of the SNMS profiles in the dissolution stage of these precipitates, we determined the concentration  $C_{\text{sat}}$  of P in equilibrium with the conjugate phase:  $C_{\text{sat}} = 2.45 \times 10^{23} \exp(-0.62/kT) \text{ cm}^{-3}$ . This concentration has to be compared with the equilibrium concentration  $n_e$  of the electrically active dopant. To this end, more accurate determinations of  $n_e$  were performed on heavily P-doped polysilicon films. It was found that  $n_e = 1.3 \times 10^{22} \exp(-0.37/kT) \text{ cm}^{-3}$ . Hence for  $T > 750$  °C,  $C_{\text{sat}}$  exceeds  $n_e$  and the concentration ( $C_{\text{sat}} - n_e$ ) of inactive mobile P increases with temperature. The formation and the diffusion behavior of this inactive dopant are in keeping with a preprecipitation phenomenon.

## I. INTRODUCTION

Phosphorus is one of the dopants more largely used in silicon device technology. The determination of the equilibrium in the Si-P binary system is important for basic knowledge, and for the comprehension of phenomena which are relevant for device technology, e.g., the annealing behavior and the diffusion processes.

In literature different SiP compounds were prepared by direct synthesis of the elements: an orthorhombic structure<sup>1</sup> and a cubic sphalerite-type one,<sup>2</sup> the latter obtained under high pressure. According to the phase diagram, below the eutectic temperature (1131 °C) and under normal pressure, the solution of phosphorus in silicon is in equilibrium with orthorhombic SiP.<sup>3</sup>

The formation of large SiP precipitates in Si is difficult; it was only obtained at very high dopant concentrations, for strong supersaturations. In slices doped by thermal predeposition precipitates mainly nucleate at the surface, adjacent to the doped oxide layer which grows during the process. In previous papers we reported the occurrence of large precipitates after predeposition at 920 and 1000 °C using  $\text{POCl}_3$ . By selected area diffraction (SAD) their structure was found to correspond to an orthorhombic one,<sup>4</sup> in agreement with the results of x-ray analysis.<sup>5</sup>

Bourret and Schröter<sup>6</sup> performed a high-resolution electron microscopy (HREM) study of SiP precipitates obtained by heavy predepositions at 900 °C using a  $\text{P}_2\text{O}_5$  source. For these precipitates they proposed a monoclinic structure, isomorphic with SiAs. Bender *et al.*<sup>7</sup> obtained a surface layer of polycrystalline SiP by annealing at 900 °C wafers implanted at extremely high fluences ( $1 \times 10^{18} \text{ cm}^{-2}$ ). These crystals presented a monoclinic structure, with a minor amount of orthorhombic phase.

The understanding of the equilibrium is further complicated by the presence of electrically inactive phosphorus. It is known that the carrier density of annealed Si crystals increases with the concentration of P, and attains an upper limit (of the order of 1 at. %) which depends on temperature,<sup>8</sup> while the total dopant can attain concentrations as high as 10 at. %.<sup>8</sup> Furthermore, it has been observed that the inactive dopant mainly occupies substitutional positions in the Si lattice.<sup>9</sup> This behavior is similar to the one presented by As in Si.<sup>10</sup>

A hypothesis to account for the inactive P was the formation of complex point defects (*E* centers) which compensate or make the dopant electrically inactive.<sup>11,12</sup> In subsequent works, we deduced that the inactive P is in the form of small coherent particles which keep the structure of the Si matrix. This conclusion was based on electrical measurements,<sup>8,13</sup> and was supported by double-crystal x-ray-diffraction<sup>14</sup> and TEM and HREM examination.<sup>8,13,15</sup> A sphalerite-type structure was proposed for these particles.<sup>15</sup>

Until now no experiment for thermal equilibration of heavily doped specimens containing clearly identified, orthorhombic or monoclinic, SiP precipitates has been performed. This is a crucial determination to analyze the phase equilibrium and the nature of the inactive P.

We recently carried out experiments of this type on As-doped Si.<sup>16,17</sup> Our determinations were performed on wafers bearing a layer of monoclinic SiAs in the surface region, obtained by annealing after very heavy As implantation (1 and  $1.5 \times 10^{17} \text{ cm}^{-2}$ ). The As concentration  $C_{\text{sat}}$  in equilibrium with this phase was determined by the shape of the diffusion profiles after equilibration at temperatures in the range 800–1050 °C.

The present work reports the results of experiments performed on the same line, by annealing very heavily

( $1.5 \times 10^{17} \text{ cm}^{-2}$ ) P-doped slices at temperatures in the range 800–1000 °C. Features of the precipitates have been studied by electron microscopy techniques. Moreover, we report more accurate values of the saturation carrier concentration  $n_e$  in the same temperature range. Finally, the equilibrium in the Si-P system and the nature of the inactive dopant are discussed in the light of these results.

## II. EXPERIMENT

Silicon wafers, (100) oriented, *p* type, of 10-Ω cm resistivity, have been phosphorus implanted with a dose  $1.5 \times 10^{17} \text{ cm}^{-2}$ . In order to increase the dopant concentration near the surface further, the process has been performed in two steps: a first implantation with a fluence  $1.0 \times 10^{17} \text{ P/cm}^2$ , at an energy of 100 keV, and followed by a second implantation with a fluence  $5 \times 10^{16} \text{ P/cm}^2$  at 50 keV.

The specimens were subsequently furnace annealed at 800, 850, 900, and 1000 °C for different times, ranging from 15 min to 160 h, in a nitrogen atmosphere. To reduce the outdiffusion of the dopant, these treatments were performed for the first 4 h at 800 °C (1 h at 850 and 900 °C, and 15 min at 1000 °C, respectively) in a slightly oxidizing atmosphere ( $\text{N}_2 + 10\% \text{-O}_2$ ).

Secondary neutral mass spectroscopy (SNMS) has been employed to measure the profiles of P concentration in Si. A Leybold INA 3 instrument has been used, with an argon plasma as the positioner source of ions to sputter the samples. To reduce ion mixing which, increasing with the primary ion energy, degrades the depth resolution, a negative voltage of 800 V was applied to the samples for sputtering. The primary current density was of about 1–2 mA/cm<sup>2</sup>.

The maximum carrier concentration  $n_e$  obtainable in heavily P-doped Si after thermal equilibration, as a function of the temperature, has been determined by a different experiment. Polycrystalline Si films were deposited in a low-pressure chemical vapor reactor at 660 °C, onto previously oxidized single-crystal wafers. The film thickness, determined by an Alpha-Step 200 Tencor Instruments, was of 0.45 μm. P was implanted in the films at an energy of 100 keV and dose  $4 \times 10^{16} \text{ cm}^{-2}$ . The samples were first heated 3 h at 1100 °C, to recover the implantation damage and redistribute the dopant, and successively annealed for 1000 h at 600 °C. To avoid outdiffusion processes the first high-temperature heat treatment was performed in a slightly oxidizing atmosphere (90%  $\text{N}_2 + 10\% \text{O}_2$ ). By using this procedure we obtain that the carrier concentration measurements performed at the end of the annealing cycle (600–1100 °C) and immediately after the first annealing (1100 °C, 3 h) gave exactly the same value. Furthermore, the poor loss of P is confirmed by a simulation of the annealing processes performed by using the process simulator SUPREM III, which gives a P loss of 1.7%. The average grain size after these thermal treatments was 1.3 μm. The specimens were then annealed at temperatures increasing in steps of 25 °C up to 900 °C, and in steps of 50 °C up to 1100 °C. The treatments were performed in a nitrogen atmosphere for times which decreased as the temperature increased, and exactly as follows: 250 h at 625, 650, 675, and 700 °C; 120 h at 725, 750, and 775 °C; 97 h at 800 °C; 50 h at 825, 850, and 875 °C; 24 h at 900, 950, and 1000 °C; 2.5 h at 1050 °C; and 1 h at

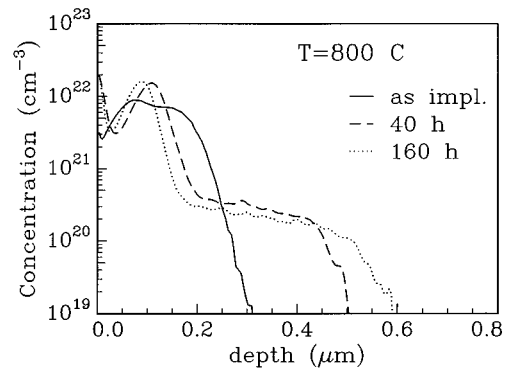


FIG. 1. SNMS phosphorus profiles after implantation and annealing at 800 °C for increasing times.

1100 °C. In order to investigate the P deactivation during the cooling, some specimens were also annealed with a rapid thermal processing system (Heat Pulse 210 T by AG Assoc.). These samples were heated at 900 and 1000 °C for 60 s and 1100 °C for 30 s, respectively, in a flowing nitrogen atmosphere.

The carrier density and mobility were determined by Hall effect and sheet resistivity measurements, using a Van der Pauw geometry defined with a photolithographic process. The carrier concentration profile in few selected specimens was determined by incremental sheet resistance and Hall effect measurements performed after thinning of the specimen by anodic oxidation and oxide stripping. Finally, for the electron microscopy observations on plan and cross sections, a Philips CM30 TEM, operating at 300 kV, has been employed.

## III. RESULTS AND DISCUSSION

### A. Dopant profiles and P concentration in equilibrium with SiP precipitates

The as-implanted P profile and its evolution during annealing at 800, 850, and 900 °C are reported in Figs. 1, 2, and 3, respectively. As shown in Fig. 1, the as-implanted distribution shows a maximum concentration slightly lower than  $1 \times 10^{22} \text{ cm}^{-3}$  at a depth of 80 nm. After annealing, the SNMS profiles reveal the presence of two distinct peaks in the P distribution. The first one, due to P segregation, is observed at the sample surface, whereas the second wider peak, attaining a concentration of about  $2 \times 10^{22} \text{ cm}^{-3}$ , a factor 2 higher than the maximum concentration in the as-implanted sample, is present at a depth of about 100 nm at 800 and 850 °C, and at a depth of about 90 nm at 900 °C. The exact position in depth of these second peaks appears to depend slightly on the annealing time.

The in-depth defect distribution in samples annealed in the above-reported temperature range has been obtained by cross-sectional TEM analysis. The bright-field (BF) TEM micrograph shown in Figs. 4(a) and 4(b) correspond to samples annealed at 850 °C for 4 h and 900 °C for 3 h, respectively. A comparison between Figs. 4(a) and 4(b) and Figs. 2 and 3 shows that in correspondence of the second peak of the P distribution a high density of precipitatelike defects is observed. Electron microdiffraction obtained from

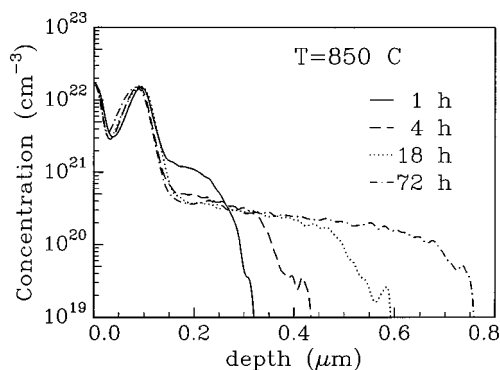


FIG. 2. SNMS phosphorus profiles after annealing at 850 °C. With increasing time the concentration diffusing from the precipitates attains a constant equilibrium value  $C_{\text{sat}}$  defined by the shoulder.

several defects have shown that they are mainly monoclinic SiP precipitates, a structure first reported by Bourret and Schroeter,<sup>6</sup> although some orthorhombic SiP precipitates, with a structure reported by Wadsten,<sup>1</sup> were also found, as shown in Fig. 5. The coexistence of the two structure of the SiP precipitates has already been reported by Bender *et al.* in Si samples implanted at higher P doses.<sup>7</sup>

In the region between the sample surface and the SiP precipitates which corresponds to the P-depleted region in the SNMS profiles, the BF images in Figs. 4(a) and 4(b) reveal the presence of a polycrystalline layer. A weak beam dark field (WBDF) micrograph of this region, taken in a sample annealed at 900 °C for 3 h, is shown in Fig. 6, where it is noted that the type of contrast of the grain labeled A is very similar to the one of the Si matrix. X-ray microanalysis performed on single grains inside the polycrystalline layer has clearly shown that most of these are Si grains, in agreement with SNMS results.

This TEM and SNMS analysis of the P distribution shows an apparently different behavior of this dopant with respect to the one observed in the case of heavy As-implanted Si.<sup>16,17</sup> In fact, whereas for As the nucleation of SiAs precipitates was found to take place uniquely at the sample surface, i.e., heterogeneously, in the present case the nucleation takes place inside the Si matrix. However, as noted above, these precipitates lie mainly at the interface between the Si matrix

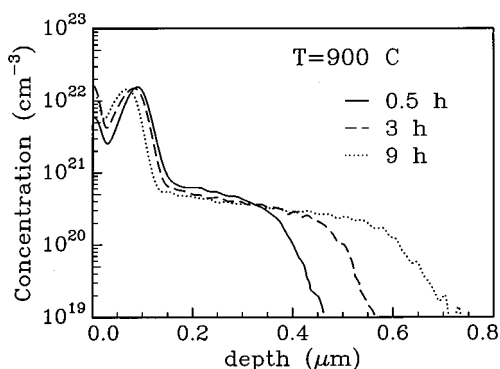


FIG. 3. SNMS phosphorus profiles after annealing at 900 °C for different times.

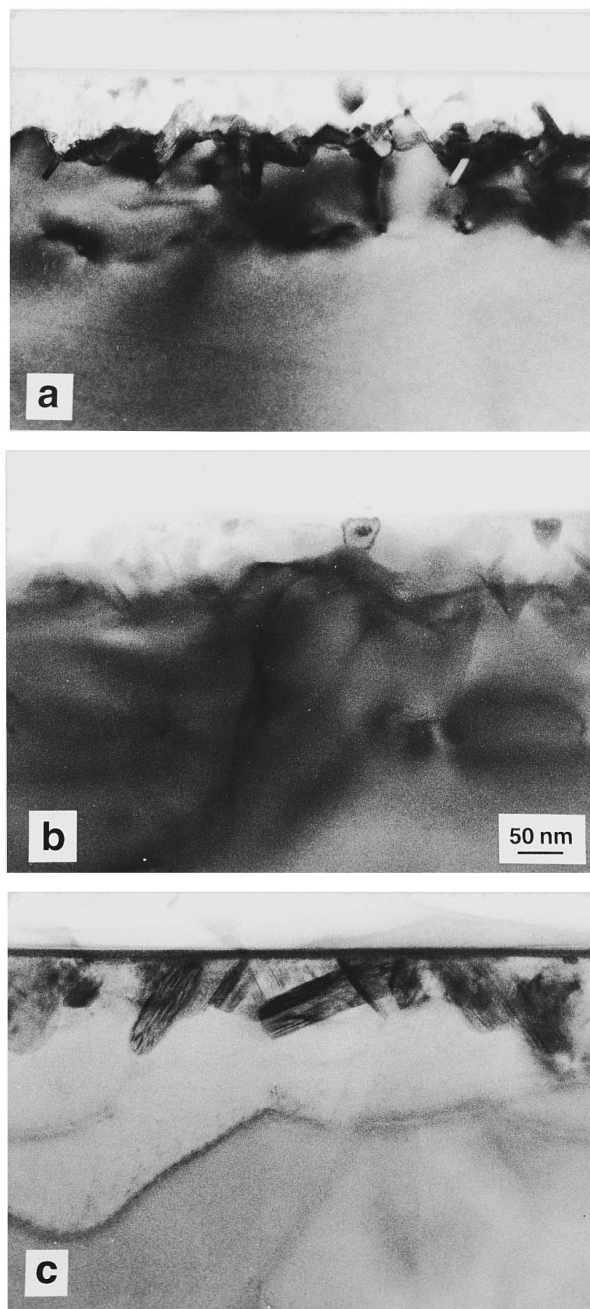


FIG. 4. BF TEM micrographs taken in specimens annealed at 850 °C for 4 h (a), 900 °C for 3 h (b), and 1000 °C for 30 min (c). The rodlike SiP precipitates are buried in (a) and to a minor extent in (b), whereas they are found at the sample surface in (c).

and the surfacial polycrystalline layer, indicating, on one hand, a heterogeneous nucleation similar to the one observed for As in Si, but, on the other hand, a different behavior of the two dopants during the solid-phase epitaxy (SPE) growth leading, in the case of P, to an imperfect regrowth of the uppermost amorphous layer (Fig. 4).

The shift of the P peak toward the surface, observed to a larger extent at 800, 850, and 900 °C (Fig. 4), by increasing the annealing time cannot be justified by the surface stripping produced by the oxidation, because the oxygen flows in the furnace only in the early phases of the annealing. A tentative explanation of this phenomenon is the Si diffusion

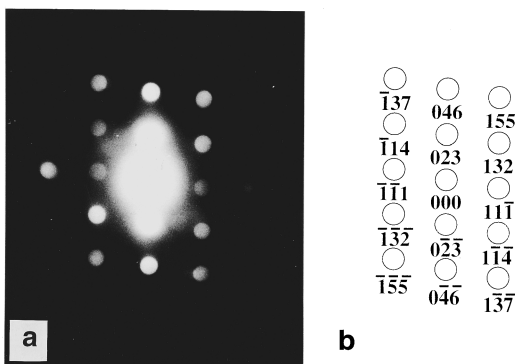


FIG. 5. (a) Microdiffraction pattern taken in a sample annealed at 1000 °C for 30 min. (b) Schematic diagram of (a) with the spots of SiP indexed, according to the [532] projection of the orthorhombic structure reported by Wadsten (Ref. 1).

from the surface polycrystalline layer toward the single-crystal bulk. The driving force for this diffusion is the free-energy difference between crystals of different sizes.

The isothermal evolution of the P distribution, as shown in Figs. 1–3, can be described as a P diffusion from the region adjacent to the SiP-rich layer both toward the precipitates, which continue to grow, and to the bulk. This process continues until the dopant concentration in the Si lattice attains the value of equilibrium with the SiP precipitates. Then the concentration stays constant, and the shoulder in the concentration profile assumes a value which represents the saturation concentration  $C_{\text{sat}}$  of P in Si. From our profiles the saturation concentration in equilibrium with orthorhombic SiP turns out to be  $3.2$ ,  $4.0$ , and  $5.4 \times 10^{20} \text{ cm}^{-3}$  at 800, 850, and 900 °C, respectively. We note that for all temperatures, the longer annealing time corresponds to a P diffusion length  $2\sqrt{Dt}$ , evaluated at the concentration  $C_{\text{sat}}$ , higher than  $1 \mu\text{m}$ .<sup>18</sup>

A different distribution is observed in the samples isothermally annealed at 1000 °C. As shown in the SNMS profile in

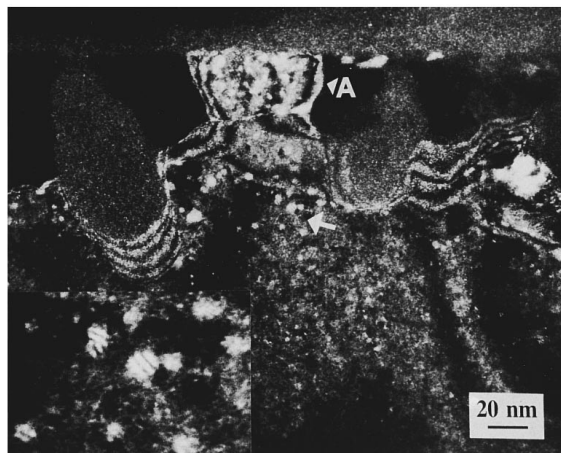


FIG. 6. WBDF ( $-g,5g$ ) micrograph taken in a sample annealed at 900 °C for 3 h, with  $g=\langle 111 \rangle$  showing a Si grain close to the surface (labeled A). In this micrograph very small particles are visible in Si regions (see arrows). In the enlarged view reported in the inset it is shown that some of these particles exhibit a Moiré fringe contrast.

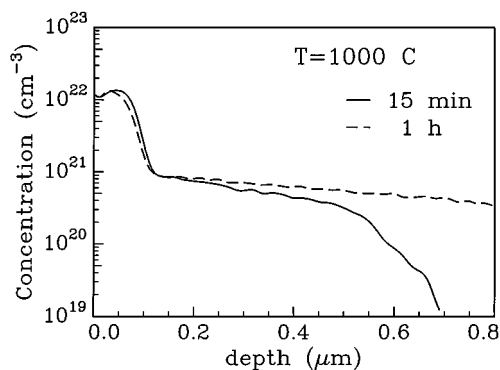


FIG. 7. SNMS phosphorus profiles showing the shoulder attaining  $C_{\text{sat}}$  after annealing at 1000 °C for increasing times.

Fig. 7, a unique peak of the P concentration is detected at the sample surface. This is confirmed by the BF TEM micrograph in Fig. 4(c), taken in a sample annealed at 1000 °C for 15 min, where large SiP precipitates are uniquely visible at the sample surface. The  $C_{\text{sat}}$  value determined from the profiles in Fig. 7 is  $9.2 \times 10^{20} \text{ cm}^{-3}$ .

To have an unambiguous confirmation that the procedure employed to obtain the P saturation concentration gives equilibrium values, we have submitted a specimen previously annealed for 160 h at 800 °C to a second thermal treatment at 900 °C for 9 h. The result of this experiment is reported in Fig. 8. The P concentration at the shoulder increases from the lower  $C_{\text{sat}}$  value attained at 800 °C to the higher one at 900 °C. This shows that the values of the P saturation concentration can be attained reversibly, thus confirming that they are the equilibrium ones.

The above results confirm that extensive precipitation of monoclinic (or orthorhombic) SiP takes place only in conditions of very high dopant supersaturation. We notice in this respect that Bender *et al.*<sup>7</sup> did not detect the above phases after annealing for 3 h at 900 °C specimens implanted with  $1 \times 10^{17} \text{ cm}^{-2}$  at 100 keV. However, after the same heat treatment, we observe their precipitation, but with a dose  $1.5 \times 10^{17} \text{ cm}^{-2}$ ; i.e., for a dopant concentration which exceeds the value of  $C_{\text{sat}}$  at 900 °C by over a factor 15. Competition between clustering and nucleation can hinder the

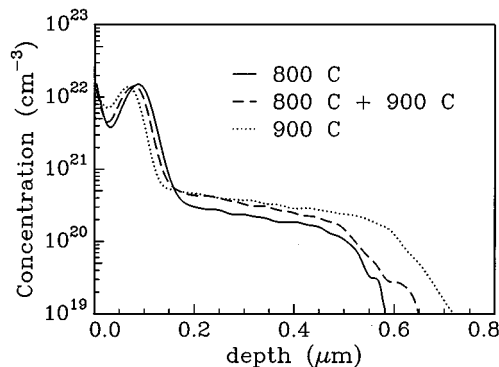


FIG. 8. Comparison of SNMS phosphorus profiles after annealing (i) at 800 °C, (ii) 800 °C and subsequently at 900 °C, and (iii) at 900 °C. After the second annealing at 900 °C the concentration of the shoulder increases from the lower  $C_{\text{sat}}$  value attained at 800 °C to the higher one of 900 °C.

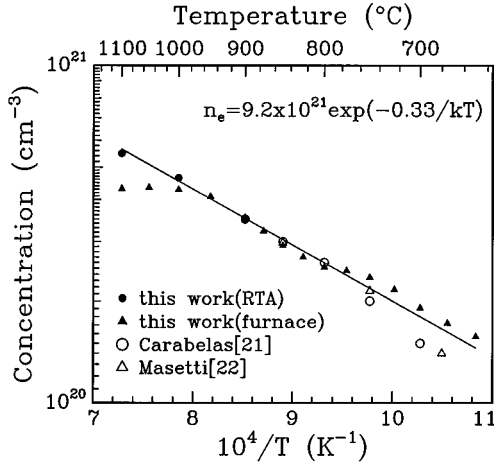


FIG. 9. Dependence on the annealing temperature of the equilibrium carrier concentration  $n_e$  measured in the specimen's furnace, and rapid thermal annealed.

kinetics of precipitation.<sup>19,20</sup> On this line the behavior of P can be attributed to competing aggregation of the dopant, i.e., to the same phenomenon which we concluded to be responsible for its electrical deactivation. A similar hindered precipitation is presented by As.<sup>17</sup>

### B. Equilibrium carrier concentration vs annealing temperature

The carrier concentration measured on our samples as a function of temperature is reported in Fig. 9, together with our previous data obtained in polysilicon films<sup>21</sup> and crystalline Si.<sup>22</sup> Although the dopant concentration in these specimens ( $\sim 9 \times 10^{20} \text{ cm}^{-3}$ ) exceeds  $C_{\text{sat}}$  only for temperatures lower than 1000 °C, it is worth noting that  $n_e$  is independent of P concentration at these extremely high dopant densities. In previous experiments we confirmed this behavior for P concentrations up to  $4 \times 10^{21} \text{ cm}^{-3}$ .<sup>8</sup>

In the low-temperature range below 800 °C, equilibrium values of the carrier density can hardly be obtained, even for long annealing times.<sup>21,22</sup> Moreover, in these experimental conditions the precipitation of orthorhombic (or monoclinic) SiP was not detected. Instead TEM WBDF observations reported evidence of a high density of small particles.<sup>13</sup> At the other extreme, at high temperatures, furnace annealing provides lower values with respect to rapid thermal annealing (RTA). The differences tend to increase with increasing temperature, and are clearly due to a dopant deactivation during cooling. This effect is minimized by RTA, which provides rapid cooling. However, at 900 °C, the furnace-annealed samples provide the same concentration values as the ones submitted to RTA.

The results reported in Fig. 9 match very well an exponential dependence as a function of reciprocal temperature. The best fit, determined leaving out the three points referring to furnace annealing at the highest temperatures, gives  $n_e = 9.2 \times 10^{21} \exp(-0.33/kT) \text{ cm}^{-3}$ .

### C. On the nature of the electrical inactive P

The dopant concentration  $C_{\text{sat}}$  in equilibrium with monoclinic SiP precipitates, and the equilibrium carrier concentra-

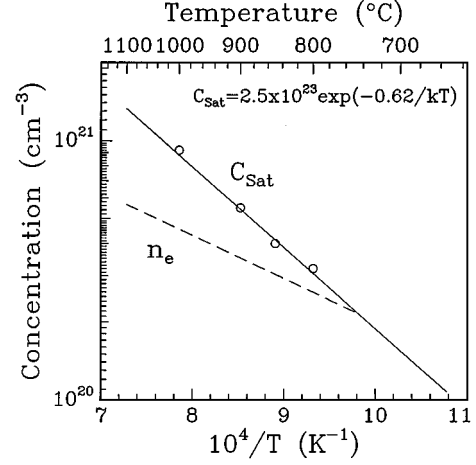


FIG. 10. Dependence on the annealing temperature of the carrier concentration  $n_e$  and the dopant concentration  $C_{\text{sat}}$  in equilibrium with SiP precipitates.

tion  $n_e$ , are reported in Fig. 10 as functions of the reciprocal temperature. The two curves, characterized by different slopes, meet at about 750 °C, corresponding to a concentration of  $2.2 \times 10^{20} \text{ cm}^{-3}$ . According to these results, above  $\sim 750$  °C, the ionized P can exist in equilibrium with both the dopant in monoclinic SiP precipitates and the inactive dopant ( $C_{\text{sat}} - n_e$ ), which can undergo diffusion.

This finding is put in clear evidence in Fig. 11, which reports the dopant and carrier profiles, in the region downstream the large SiP precipitates, after 15 min of annealing at 1000 °C. We point out that the value of the concentration in the plateau region of the carrier profile closely corresponds to the one in Fig. 10. Moreover, the P and carrier profiles overlap for concentrations lower than  $3 \times 10^{20} \text{ cm}^{-3}$ . This is an indication of the accuracy of our measurements. Qualitatively similar behavior was also observed for As.<sup>16,17</sup> For this last element the fraction of inactive mobile dopant is higher than in the case of P. In fact, it can exceed the electrically active one by more than one order of magnitude.<sup>17</sup>

An alternative hypothesis is that the formation of inactive P at concentrations lower than  $C_{\text{sat}}$ , as is shown in Fig. 10

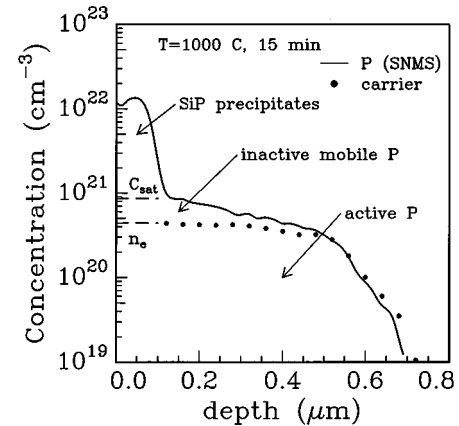


FIG. 11. Phosphorus and carrier profiles after 15-min annealing at 1000 °C.

for  $T > 750^\circ\text{C}$ , is merely due to deactivation taking place during cooling. However, this hypothesis is in contrast with the results of Fig. 9 (same carrier concentration for the samples heated at  $900^\circ\text{C}$  both by furnace and RTA), and with the following findings.

(i) Equilibration annealing at  $1000^\circ\text{C}$  was performed on both polycrystal and single-crystal specimens by using different heating and cooling techniques. The spread of our results for  $n_e$ , also considering our previous determinations,<sup>8,19</sup> is in the range  $3.8/(4.6 \times 10^{20} \text{ cm}^{-3})$ , where the highest figure was obtained by RTA followed by rapid cooling in a nitrogen flux. These values have to be compared with the one of  $C_{\text{sat}}$ , i.e.,  $9.2 \times 10^{20} \text{ cm}^{-3}$ .

(ii) Determinations of the carrier profiles, after heating heavily doped laser annealed samples at  $850^\circ\text{C}$ , have shown that heating times exceeding 5 min are needed to obtain the equilibrium value ( $n_e = 2.9 \times 10^{20} \text{ cm}^{-3}$ ).<sup>8</sup>

(iii) The analysis of the deactivation kinetics<sup>13</sup> indicates that the rate of this process decreases strongly with decreasing supersaturation. Instead, the carrier profiles, like the one of Fig. 11, present a wide, nearly flat, region.

According to the results in Figs. 10 and 11, the inactive dopant at concentrations below  $C_{\text{sat}}$  should be due to an aggregation phenomenon which precedes the phase transition. In these heterophase fluctuations, first analyzed by Frenkel,<sup>23</sup> the population of embryos is in a mass action equilibrium with the parent monomer. Such an equilibrium can account for the diffusion behavior, such as the one shown in Fig. 11, for the inactive dopant.

Finally, we have found that, as in the case of heavy As-implanted Si,<sup>17</sup> in addition to large second-phase precipitates small particles are detected in WBDF observations. In the present case, as shown in Fig. 6, they are observed both inside the surfacial Si grains and deeper in the substrate, i.e., at concentrations below  $C_{\text{sat}}$ , with diameters ranging from

1.5 to 7.5 nm. In the inset in Fig. 6, it is shown that in some cases they present a Moiré fringe contrast with fringe spacing ranging from 0.9 to 1.6 nm. A detailed analysis on the origin of these Moiré patterns is in progress. Presently, although some features of these small objects suggest that they are related to P, no certain conclusion can be inferred.

#### IV. CONCLUSIONS

We have determined values of the P concentration in Si in equilibrium with large monoclinic (or orthorhombic) SiP precipitates as a function of the temperature  $C_{\text{sat}} = 2.45 \times 10^{23} \exp(-0.62/kT) \text{ cm}^{-3}$ . These concentration values have been compared with the equilibrium concentration  $n_e$  of the electrically active dopant. To this end, more accurate determinations of  $n_e$  were performed on heavily P-doped polysilicon films. It has been found that  $n_e = 1.3 \times 10^{22} \exp(-0.37/kT) \text{ cm}^{-3}$ .

For temperatures higher than  $750^\circ\text{C}$ ,  $C_{\text{sat}}$  exceeds  $n_e$ . The concentration ( $C_{\text{sat}} - n_e$ ) of the inactive and mobile P increases with temperature: at  $1000^\circ\text{C}$  about 50% of the P in equilibrium with the SiP precipitates (i.e.,  $\sim 5 \times 10^{20} \text{ cm}^{-3}$ ) is electrically inactive.

This inactive mobile dopant should be due to an aggregation phenomenon which precedes the phase transition. In these heterophase fluctuations the population of embryos is in a mass action equilibrium with the parent monomer. Such an equilibrium can account for the diffusion behavior and the electrical inactivity of the dopant.

#### ACKNOWLEDGMENTS

The authors wish to thank F. Corticelli, D. Govoni, P. Lazzari, G. Pizzochero, and P. Negrini for technical assistance.

- <sup>1</sup>T. Wadsten, *Chem. Scr.* **8**, 63 (1975).
- <sup>2</sup>J. Osugi, R. Namikawa, and J. Tanaka, *Rev. Phys. Chem. Jpn.* **36**, 35 (1966).
- <sup>3</sup>R. W. Olesinsky, N. Kanani, and G. J. Abbaschian, *Bull. Alloy Phase Diagrams* **6**, 130 (1986).
- <sup>4</sup>A. Armigliato, D. Nobili, M. Servidori, and S. Solmi, *J. Appl. Phys.* **47**, 5489 (1977).
- <sup>5</sup>M. Servidori and A. Armigliato, *J. Mater. Sci.* **10**, 306 (1975).
- <sup>6</sup>A. Bourret and W. Schröter, *Ultramicroscopy* **14**, 97 (1984).
- <sup>7</sup>H. Bender, D. Avau, W. Vandervost, J. Van Landuyt, and H. E. Maes, *Mater. Sci. Forum* **10-12**, 1165 (1986).
- <sup>8</sup>D. Nobili, A. Armigliato, M. Finetti, and S. Solmi, *J. Appl. Phys.* **53**, 1484 (1982).
- <sup>9</sup>E. Fogarassy, R. Stuck, J. C. Muller, A. Grob, J. J. Grob, and P. Siffert, *J. Electron. Mater.* **9**, 1977 (1980).
- <sup>10</sup>D. Nobili, A. Carabelas, G. Celotti, and S. Solmi, *J. Electrochem. Soc.* **130**, 922 (1983).
- <sup>11</sup>D. L. Kendall and R. Carpio (unpublished).
- <sup>12</sup>R. B. Fair and J. C. C. Tsai, *J. Electrochem. Soc.* **124**, 1102 (1977).
- <sup>13</sup>M. Finetti, P. Negrini, S. Solmi, and D. Nobili, *J. Electrochem. Soc.* **128**, 1313 (1981).
- <sup>14</sup>M. Servidori, C. Dal Monte, and Q. Zini, *Phys. Status Solidi A* **80**, 277 (1983).
- <sup>15</sup>A. Armigliato and P. Werner, *Ultramicroscopy* **15**, 61 (1984).
- <sup>16</sup>A. Parisini, D. Nobili, A. Armigliato, M. Derdour, L. Moro, and S. Solmi, *Appl. Phys. A* **54**, 221 (1992).
- <sup>17</sup>D. Nobili, S. Solmi, A. Parisini, M. Derdour, A. Armigliato, and L. Moro, *Phys. Rev. B* **49**, 2477 (1994).
- <sup>18</sup>R. B. Fair, in *Silicon Integrated Circuits*, edited by D. Kahng (Academic, New York, 1981), p. 1.
- <sup>19</sup>J. L. Katz, H. Salsburg, and H. Reiss, *J. Colloid Interf. Sci.* **21**, 560 (1966).
- <sup>20</sup>R. D. Doherty, in *Physical Metallurgy*, edited by R. W. Cahn and P. Haasen (North-Holland, Amsterdam, 1983), pp. 934-1029.
- <sup>21</sup>A. Carabelas, D. Nobili, and S. Solmi, *J. Phys. (Paris)* **43**, C187 (1982).
- <sup>22</sup>G. Masetti, D. Nobili, and S. Solmi, in *Semiconductor Silicon 1977*, edited by H. R. Huff and E. Sirtl (Electrochemical Society, Princeton, 1977), p. 648.
- <sup>23</sup>J. Frenkel, *Kinetics Theory of Liquids* (Dover, New York, 1955).